

A COMPARATIVE ANALYSIS OF PARTICLE - MIXING PLANE INTERACTION IN MULTISTAGE TURBOMACHINERY SIMULATIONS

S. Oliani¹, R. Friso, N. Casari, M. Pinelli, A. Suman

Department of Engineering, University of Ferrara, Via Saragat, 1, Ferrara (IT), 44122

M. Carnevale

Department of Mechanical Engineering, University of Bath, Bath, BA2 7AY, United Kingdom

ABSTRACT

Rotor-stator interaction in turbomachinery is one of the most challenging fields in Computational Fluid Dynamics (CFD) and, in this regard, several studies can be found in the literature, concerning unsteady coupling of successive blade rows. The mixing plane for steady multistage calculations has been common for many years and, even though this technique is at present consolidated, the proper way of handling multiphase flows is not well defined. Currently, only a few particle-interface interaction studies are reported in the literature, hence strong limitations in particle-laden flow simulations in multistage turbomachinery arises. In order to fill up this lack, this work reports an analysis for particle-mixing plane interaction. Efforts have been done to supplement the Lagrangian tracking library of the open-source software *foam-extend* with an appropriate treatment of particles crossing mixing plane interfaces. The component analysed in this work is the first high-pressure stage of an Energy-Efficient Engine (EEE) axial turbine. The results of the study is compared to high-fidelity results obtained by a transient simulation based on a dynamic mesh approach. Three different techniques have been proposed and their performance has been assessed. One of the three methods has proved superior to the others in capturing the time-averaged effects of the unsteady flow on particle impacts and is therefore suitable when performing steady-state simulations.

KEYWORDS

MIXING-PLANE METHOD, CFD, AXIAL TURBINE, DISPERSE-FLOWS

NOMENCLATURE

c vane/blade chord	x Axial coordinate along the chord
C_p pressure coefficient	r_p Particle position
d_p particle diameter	η_{imp} Impact efficiency
F_{centr} centrifugal force	Ω Angular velocity
F_{Co} Coriolis force	ARD Arizona road dust
m_p particle mass	BBO Basset-Boussinesq-Oseen equation
p pressure	CFD Computational fluid dynamics
p_0 total inlet pressure	EEE Energy Efficient Engine
T_0 total inlet temperature	GGI General Grid Interface
T_{wall} Temperature at blade/vane surface	GT Gas turbine
v_p particle velocity	

INTRODUCTION

In modern industrial applications, turbomachinery flows are often dispersed with particles like solid contaminants or water droplets, just to name a few. These contaminants are often undesired since they can cause degradation of internal surfaces. Computational Fluid Dynamics (CFD) simulations represent an increasingly used tool for the design and diagnosis of the components that operate in these critical conditions. To be suitable for industrial purposes, the time to carry out these computations need to be sufficiently small. In this regard, several efforts have been done by the scientific community to reduce the computational burden by proposing new models. Among the others, one of the most common methods is the mixing-plane, which tries to overcome the problem of the interaction between static and moving components. Even though this technique is at present consolidated, it still represents a challenge when this strategy is used in particle-laden flows simulations. In this paper, the specific issue of solid contaminants entering Gas Turbines (GTs) has been chosen as a representative problematic situation. In the aeronautic industry, the presence of particles into the engine is of increasing importance to operators and equipment manufacturers (see for example Prenter et al. (2017)). Particles entering the engine can deposit and/or erode internal surfaces, thus reducing the lifetime of components. Since GTs are multistage turbomachinery, the mixing-plane strategy is fundamental to avoid extremely high computational time. Despite the presence in the literature of several works investigating particles effects in multistage turbomachinery (e.g. Corsini et al. (2013); Suman et al. (2014)), it is the impression of the authors that a thorough assessment of the models has not been carried out yet. This limits the reliability of this kind of simulation, and this work tries to systematically investigate pros and cons of different approaches. To date, a number of multistage simulation including discrete-phase presence has been performed. For example, Ghenaiet (2014) studied particle ingestion in a two-stage gas turbine for erosion analysis using a frozen rotor, multiple reference frame model. On the other hand, Yang and Boulanger (2012); Suzuki et al. (2006) tracked particles in frozen flow fields obtained from unsteady simulations with a consequent large computational time. In consideration of this issue, Zagnoli et al. (2015) used a mixing-plane interface and studied two different particle averaging techniques: averaged and preserved. The first method broke up the vane exit into radial bands, averaging all the particle properties in each of them and assigning those averaged values to each particle within the respective band. The second method preserved each particle properties but randomly assigned a new circumferential coordinate. They found that no significant differences are yielded from the two methods.

In the present paper, the authors tried to push the investigation forward. Three particle-interface interaction methods have been proposed, comparing their prediction capabilities to a high-fidelity transient simulation based on the sliding mesh approach. The first stage of the high-pressure turbine of the General Electric Energy Efficient Engine (EEE) analysed by Thulin et al. (1982) is considered as the reference geometry. All the simulations have been performed with the open-source software foam-extend-4.1, and efforts have been done to implement an extended interface treatment for Eulerian-Lagrangian simulations. To be more general as possible, the results are presented in terms of particle impact efficiencies on the vane and rotor blade. The aim of this work is to find a particle-mixing plane interaction method suitable to capture the time-averaged behaviour of particle impacts on blade surfaces. This is of crucial importance in particle-laden flows since unsteady calculations typically need a considerable computational effort, and one has often to resort to steady-state simulations to obtain results in an acceptable turnaround time.

The techniques for particle tracking through mixing plane interfaces were implemented from scratch in the foam-extend software and are readily applicable to any kind of turbomachinery flow. For a thorough discussion of the implementation the reader is referred to Oliani et al. (2021).

METHODOLOGY AND FLOW FIELD VALIDATION

Geometry and Computational Domain

In this study, the first stage of the EEE high-pressure turbine is considered as a reference geometry for GT applications. The whole annulus 3D configuration has been modified for exploiting periodicity properties. The actual number of vanes and rotor blades in the experiment (24 and 54, respectively) has been changed to obtain a 1 : 2 ratio (25 and 50). In this way, the simulations could be carried out in a one-vane/two-blades domain. The cooling system was not taken into consideration, not to introduce further complexity in the numerical analysis. The computational domain extends one vane chord upstream of the inlet section and one blade chord downstream from the stage exit (see Fig. 1). A fully structured hexahedral grid of nearly 3.3 million cells was generated using ANSYS TurboGrid. Furthermore, cells refinement close to the walls has been introduced to resolve the near-wall region according to the selected turbulence model (see below). The growth rate of the prism layers was set in such a way to provide an average wall $y^+ \approx 1$ and everywhere lower than 5.

Solution methods

The numerical resolution of the particle-laden flow starts with the computation of the continuous phase, which is clean airflow without solid particles. This phase was modelled by the Favre-averaged Navier-Stokes equations. The explicit density-based solver *transonicMRFDyM-Foam* developed by Borm et al. (2011) was used for the numerical solution. It adopts the *hllc* approximate Riemann solver to compute inviscid fluxes, while the viscous term is treated with a central difference approximation. Second-order accuracy in space is obtained reconstructing the variables according to the MUSCL approach, with the Van Albada slope limiter. The solver was implemented in the open-source software foam-extend-4.1. For the steady simulations, a *pseudo* time stepping approach combined with a 4-step Runge-Kutta integration was used, while a *dual time stepping* method was exploited to solve the unsteady problem. In the unsteady case, second order accuracy in time was also achieved using a three-time levels backward Euler scheme.

The operating conditions considered for the study reproduce the design point described by the technical report by Thulin et al. (1982). At the inlet of the domain, uniform total pressure and temperature equal to $p_0 = 13.25$ bar and $T_0 = 1633$ K respectively have been imposed. Besides, the turbulence intensity at the inlet of the vane passage has been set to 5 %. The effects of turbulence were computed by the *shear stress transport k- ω* (SST) model, either for the steady (RANS) and unsteady (URANS) framework. A temperature of $T_{wall} = 1100$ K has been imposed at the domain walls to approximate the coolant injection effect. Finally, a static pressure of $p = 2.75$ bar has been set at the outlet of the domain, in order to guarantee an absolute isentropic exit Mach number of

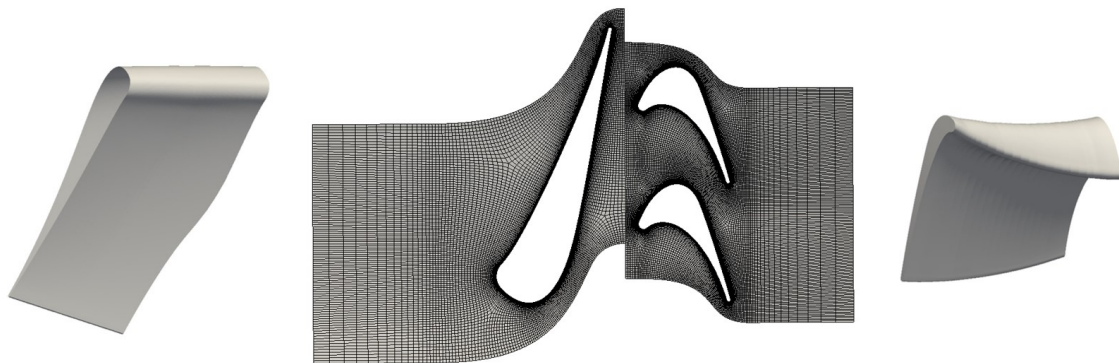


Figure 1: Computational domain.

0.52 as reported in the technical report. For the steady calculations, the mixing-plane approach has been used. This has been implemented in foam-extend software by Jasak and Beaudoin (2011) as an evolution of the Generic Grid Interface (GGI). Since the purpose of the paper is to compare several types of treatments of solid particles at mixing-plane interface, the authors have chosen a transient simulation as a high fidelity reference for the comparison. The sliding-mesh approach makes use of an overlapGGI interface to preserve fluxes between the two rows. In this way the transient interaction between the stationary and rotational domains is accounted for.

Once the flow field was solved, particles were seeded from the inlet of the domain with a uniform distribution. Aware of the large variety of solid particles that can enter the engine, the authors have chosen the Arizona Road Dust (ARD), which is one of the most common and tested in the literature, see Reagle et al. (2014). The choice was guided by considering the possible reproducibility of the results in experimental test rigs, and to maximize the generalization of the outcomes. The particle size distribution has been divided into 8 discrete sub-diameters starting from 1 μm and growing with a power of two until 128 μm . The amount of particles injected is derived with the aim of obtaining a statistically meaningful representation of the impacts. A number of 100,000 particles for each diameter has been chosen by the authors. Particle trajectories were computed by integrating the Basset-Boussinesq-Oseen (BBO) equation for each of them. The only relevant force to be kept into account is the drag, since other forces are at least one order of magnitude smaller, as suggested by Rispoli et al. (2015). For steady-state simulations, particles are tracked in a relative reference of frame and centrifugal and Coriolis non-inertial forces are added to the equation of motion. The magnitude of these forces is set to zero in the statoric domain, while in the rotating part they are respectively defined as

$$\mathbf{F}_{\text{centr}} = -m_p \boldsymbol{\Omega} \times \boldsymbol{\Omega} \times \mathbf{r}_p \quad (1)$$

$$\mathbf{F}_{\text{Cor}} = -2m_p \boldsymbol{\Omega} \times \mathbf{v}_p \quad (2)$$

where $\boldsymbol{\Omega}$ is the angular velocity of the rotating frame. The maximum particle volume fraction is small enough to model the interaction between particles and fluid flow with the one-way coupling, according to Elghobashi (1994). Particles are tracked through the domain until they escape from the outlet. The impact behaviour was modelled using the rebound model proposed by Reagle et al. (2014), where normal velocity and impact angle are used to compute the restitution coefficients. Finally, to account for the effect of turbulent dispersion on particles, the Discrete Random Walk Model of Gosman and Ioannides (1983) has been used.

Flow Field Validation

The technical report by Leach (1983) was taken as reference for either vane and rotor validation. Concerning the vane, the pressure coefficient C_p has been adopted to compare the numerical results to the experimental ones. The outcome of the comparison is reported in Fig. 2 a). In this figure the C_p profile along the vane mid-span from the steady mixing plane simulation is depicted. As can be seen, good matching has been reached for this section, even if some difference is present at the trailing edge. Regarding the rotor, no blade pressure measurements are available in the test report. To overcome this issue, the validation of the blade was conducted comparing the exit flow angles at the outlet of the domain. The results are reported in Fig. 2 b), where labels have been added to the original experimental contours to ease the comprehension. As can be noted, the general spanwise trend and contour shapes of the experimental measures are captured by the steady-state simulation. Moreover, the same solver *transonicMRFDyMFoam* was also validated elsewhere (see Borm et al. (2011)) and has been used to perform both the steady as well as the transient computations. For this reason the solution is considered validated also for the unsteady case.

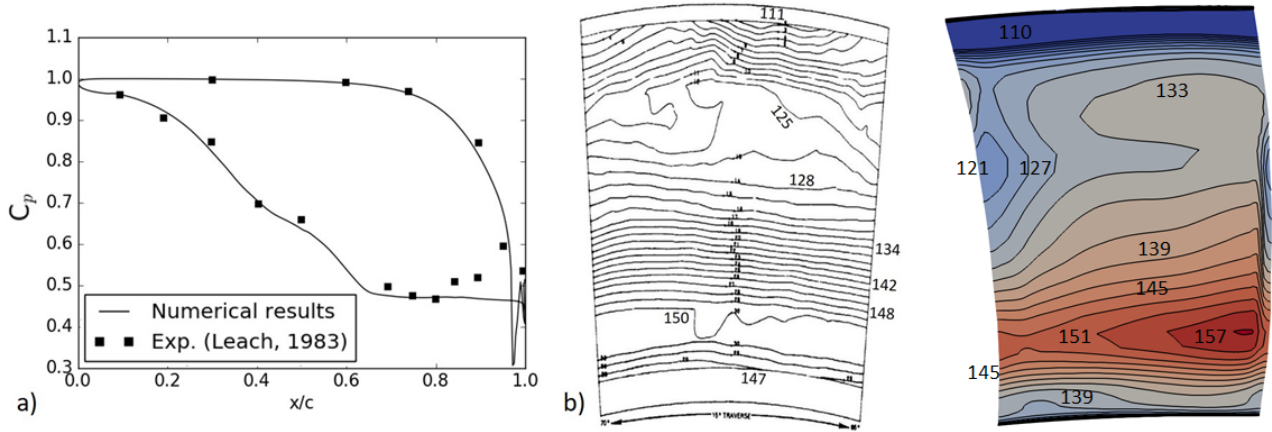


Figure 2: Numerical validation results: C_p evolution along the mid-span a) and rotor exit flow angles b).

DISCRETE-PHASE TREATMENT AT THE INTERFACE

The main purpose of this work is to compare three particles-mixing plane interaction models to an high-fidelity transient simulation. A novel particle-interface support has been implemented in foam-extend, allowing the passage of particles through different kind of coupled interfaces such as mixing planes and GGIs. The particle passage through interfaces hinges upon the face addressing between the two coupled sides. Therefore, there is no preferential crossing direction of the interface, making the algorithm robust with respect to separation bubbles and reverse flows between the blade rows. Besides, three types of discrete-phase treatments at the interface have been introduced in the computational routine, as will now be shown. The chosen techniques are based on different easiness of implementation and physical soundness:

- no redistribution (noRed): no particle redistribution and no particle velocity changes through the mixing plane interface (frozen rotor-like model);
- circumferential redistribution (crcRed): particles are circumferentially redistributed along the interface, but no particle velocity changes occur through the mixing plane. Here, the particles approaching the interface will be redistributed randomly inside each of the stripes created by the mixing plane algorithm;
- circumferential redistribution with new velocity value assigned (crcVelRed): particles are circumferentially redistributed after the mixing plane (like in the crcRed), and the velocity of each particle is set equal to the mixed-out fluid velocity in the rotating frame of reference of the correspondent stripe;

noRed and crcRed have already been used in previous frozen rotor and mixing plane simulations (see the "INTRODUCTION" section), while crcVelRed is a new type of model, aiming to simulate a full mixed-out state, where particles are at the equilibrium with the surrounding fluid. Once they cross the interface, particles are tracked into the relative frame of reference of the blade domain using the relative velocity. Since for GTs deposition and erosion are the most dangerous consequences of particles ingestion, the distribution of the impacts on the wall surfaces was chosen as the reference parameter for the comparison.

Regarding the unsteady simulation, a sliding mesh approach is used and particle trajectories are tracked in a continuous manner across the interface. The complete transient particle-laden

flow through the entire stage has been computed with a pretty fine time step of $10^{-7}s$. This was necessary to provide accurate particles trajectory all the way through the domain, due to the importance of mesh motion effects.

RESULTS

In this section, the comparison between the transient and the three steady simulations has been carried out. Specifically, with the term *steady* we refer to the case in which the flow field is firstly computed with a steady-state calculation (mixing plane) and then the particles are injected and tracked all the way through the domain in a single Lagrangian step. On the other hand, the term *transient* denotes a simulation in which the Eulerian (flow) step and the Lagrangian (particles) step alternate themselves during the solution. In this way, particles trajectories are evolved of a small dt at the end of each Eulerian. It is clear that the transient case is much more computationally expensive than the steady case, since the flow field has to be updated continuously after particle injection to account for unsteady effects on their trajectory. Firstly, critical assessment of the proposed methods for particle-mixing plane interaction has been reported in terms of impact efficiency and impact areas and compared with one another (Fig.3). Then, each method has been compared with the results from the transient simulation, in order to establish which one performs the best (Fig.7).

Impact efficiency

The first parameter the authors considered is the impact efficiency (η_{imp}), that is the number of impacted particles over the total particles injected for each diameter. Impact efficiencies for the three explored methods against the particle diameter has been reported in Figure 3 for either the vane and the blade. As can be seen, in both cases there are efficiencies greater than one. This is due to particles that impact walls more then once, leading to a total count of impacts greater than the total amount of particles injected. Concerning the vane surface, Figure 3a) shows extremely good agreement between the various types of redistribution. This is expected since the only difference on vane impacts is due to the larger particles that rebound from the blade row back to the statoric row. These particles interact twice with the mixing plane: once when they cross the

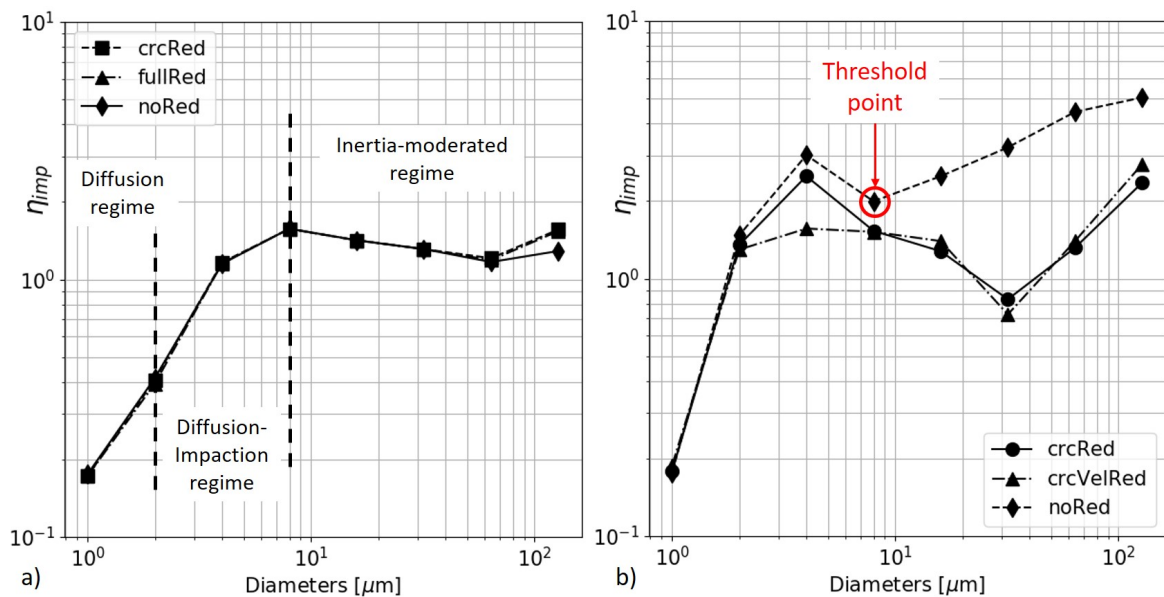


Figure 3: Impact efficiency evolution along vane a) and rotor b) varying the particle diameter.

interface forward and once backward. This effect causes slightly different impacts for very large particles, as can be noticed for $64\mu m$ and $128\mu m$ diameters in Fig. 3a). The authors noted that the trend shown in this figure is similar to the one reported in the experiments of Liu and Agarwal (1974), where turbulent deposition in a straight pipe was caught. As in the experiments, also here three different regimes such as diffusion ($d_p < 2\mu m$), diffusion-impaction ($2\mu m < d_p < 8\mu m$) and inertia-moderated ($d_p > 8\mu m$) can be highlighted (Forsyth et al. (2016)). These three regimes distinguish three different physical mechanisms of impact, which hinge upon particles inertial characteristics (larger the inertia greater the impact efficiency). On the other hand, the rotating component presents a more complex behaviour compared to the stationary one. As can be noted in Fig. 3 b), the rotor is very sensitive to the specific technique used for the interface treatment. Analyzing the different effects of redistribution and mixed-out fluid velocity assignment, the authors found a sort of threshold point (see Figure 3 b)): when particle diameter is less or equal to $8\mu m$ (diffusion regime), *crcVelRed*, *crcRed* and *noRed* lead to similar impact efficiencies; When particles diameter is greater than $8\mu m$ (inertia-moderated regimes), the results of the *crcRed* and *noRed* tend to follow the same trend, while the *crcVelRed* shows significant difference as the diameter increase. Therefore, from a global-impacts count perspective, the velocity of the particles downstream of the mixing plane becomes the most important factor affecting their behaviour when inertial properties become important. On the other hand, very small particles will rapidly settle to fluid velocity, and therefore the preservation or not of their velocity across the interface has not a major effect.

Impact areas

Since the impacts on stationary component were not appreciably influenced by the interface treatment, major attention has been paid to the rotating component for the analysis of impact areas.

In Fig. 4 the comparison of the three different discrete-phase treatments at the interface has been reported. Particles diameters have been grouped into three ranges: $(1 - 4)\mu m$, $(8 - 32)\mu m$ and $(64 - 128)\mu m$. In the figure, pictures laying in the same column have been subjected to the same treatment, and pictures laying in the same row pertain to the same particle diameter range. It is worth noting that particles impacts with the *noRed* technique will necessarily show a dependency on the vane-blade clocking. For this reason, both blades are reported in the corresponding column. When a redistribution is applied, this dependence vanishes leading to the same impact areas for the two blades. As can be seen, when small particles are injected, impacts count and areas do not change significantly (first row). Naturally, this consideration holds true for the average impacts between the two blades in the *noRed* case. On the other hand, when diameter increases, impact efficiency magnitudes and areas change between the different methods. Specifically, while *crcRed* and *noRed* find agreement in terms of impact efficiency and patterns, *crcVelRed* seems to over-predict both the characteristics (larger areas and impacts). Again, this difference between the proposed techniques is mainly due to the velocity of particles downstream of the interfaces. When the *crcVelRed* method is used, all the particles lying on the same strip are given the same velocity (the corresponding mixed-out fluid velocity in the strip) and their trajectory is significantly modified. Indeed, when the velocity is maintained across the interface, larger particles will have a negative incidence angle relative to the rotor blade. As noticed also by Tabakoff et al. (1991), this is due to the fact that the acceleration of bigger particles in the stator is not as high as for the smallest ones, thus strongly reducing the incidence direction of particles approaching the blade row. This effect is wiped out when *crcVelRed* is applied because particles velocity at the inlet of the rotating component is forced to be equal to fluid velocity. Besides, it can be noted also that as the particles diameter increases, the impact zones shift toward the tip area of the blade

due to centrifugal effect. This result has been also found by Tabakoff et al. (1991), where the effects of particles size on a turbine stage has been studied. As in the present work, they noticed that larger particles undergo a greater amount of impacts with the blade surface. Moreover, large

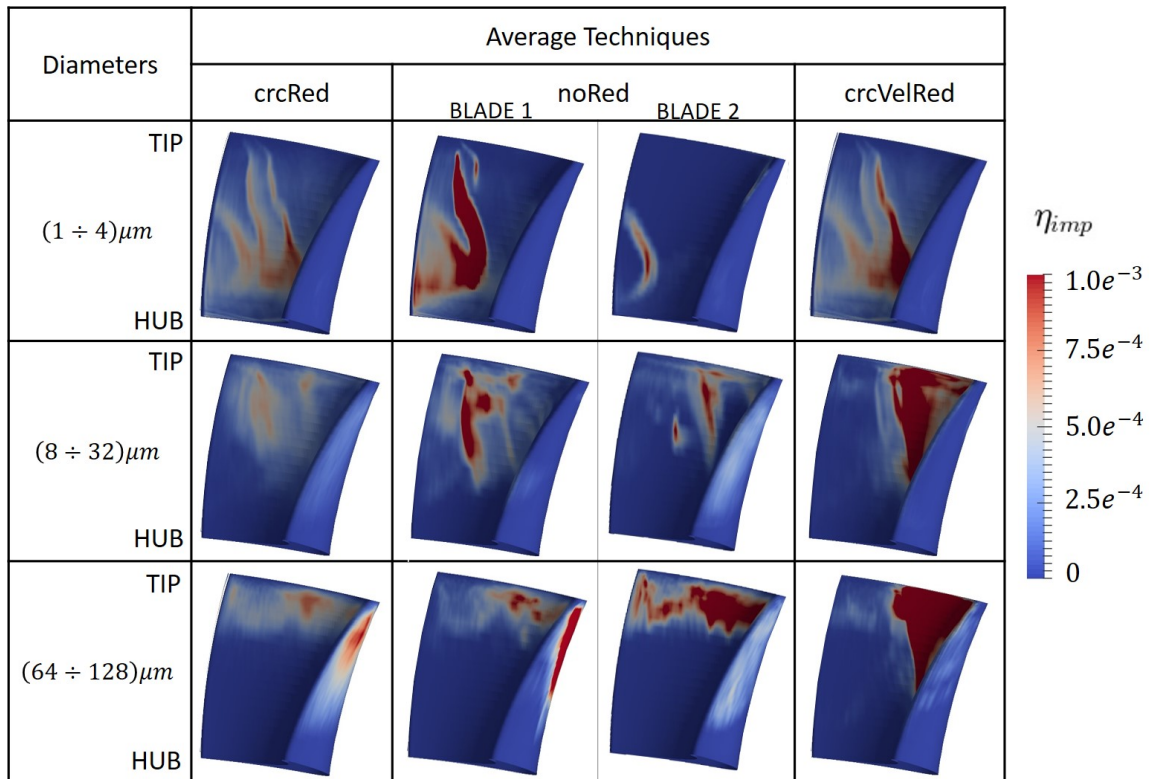


Figure 4: Impact areas on blade surface.

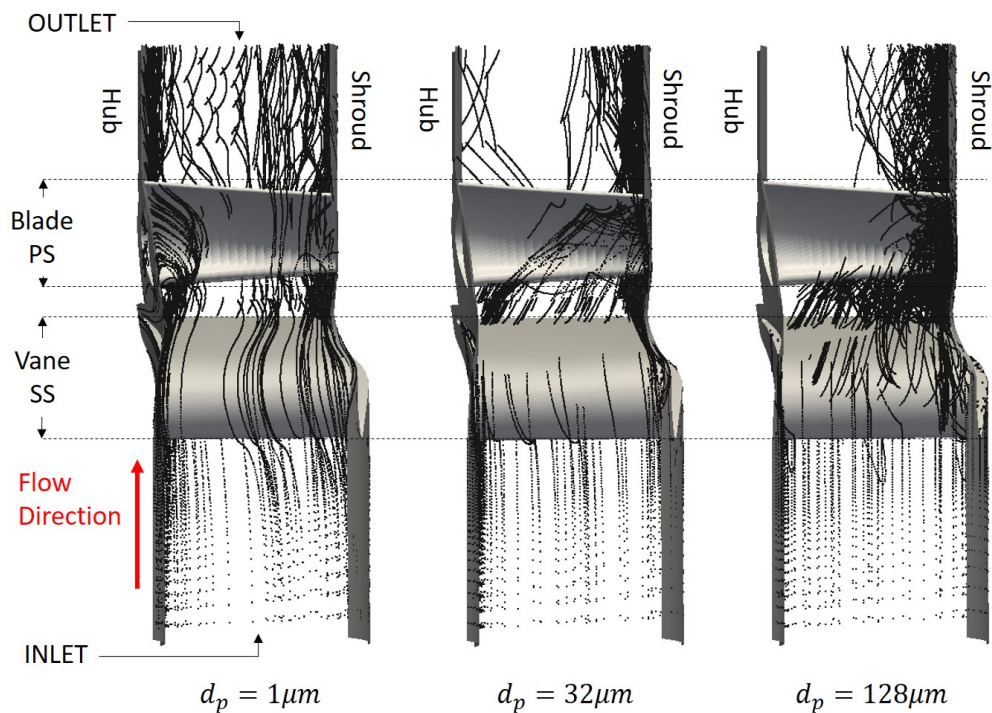


Figure 5: Particles trajectories through the domain varying particles diameter.

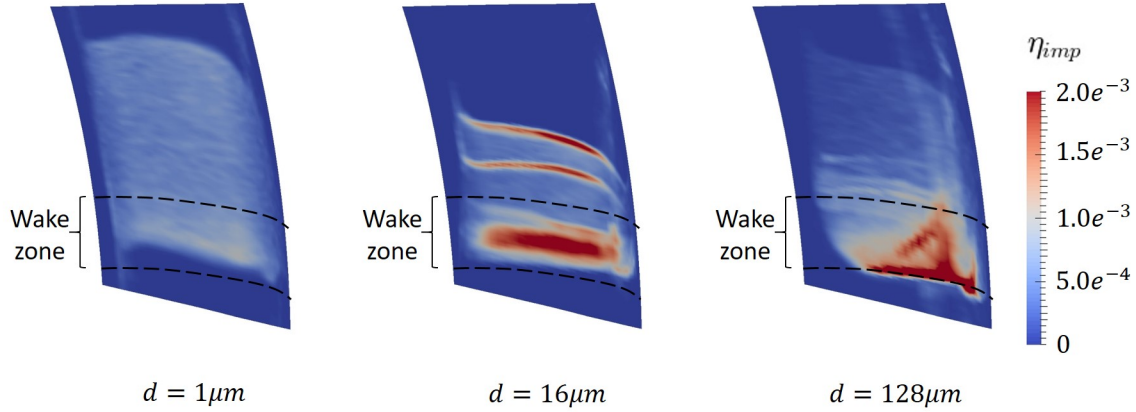


Figure 6: Impact efficiency on the interface for small ($1\mu m$), medium ($16\mu m$), and large ($128\mu m$) diameters.

particles centrifuge faster after they impact the rotor blade suction surface near the leading edge, as shown in Fig. 5 where the trajectories along the domain in the noRed case have been reported as an example. Consider now the influence of the vane wake on the particle distribution at the interface. Since the flow is far from being uniform at that area, the redistribution forces the particles to spread uniformly in the circumferential direction. To illustrate this effect, the distribution at the vane interface for the noRed case is reported in Fig. 6, where dashed lines are introduced to highlight the wake region. As can be seen, smaller particles ($1\mu m$) have a more span-wise uniform distribution, while medium-sized ($16\mu m$) and larger particles tend to gravitate towards the wake, heavily influencing their position on the interface. These results are useful to understand how strong the hypothesis behind particles redistribution at the mixing-plane is. Anyway, this doesn't mean that such a technique is not able to capture the average effect over one blade passing period.

Steady and transient comparison

In this section, the comparison between the transient simulation and steady-state results has been reported. Similarly to the previous section, the trend of the global impact efficiency in func-

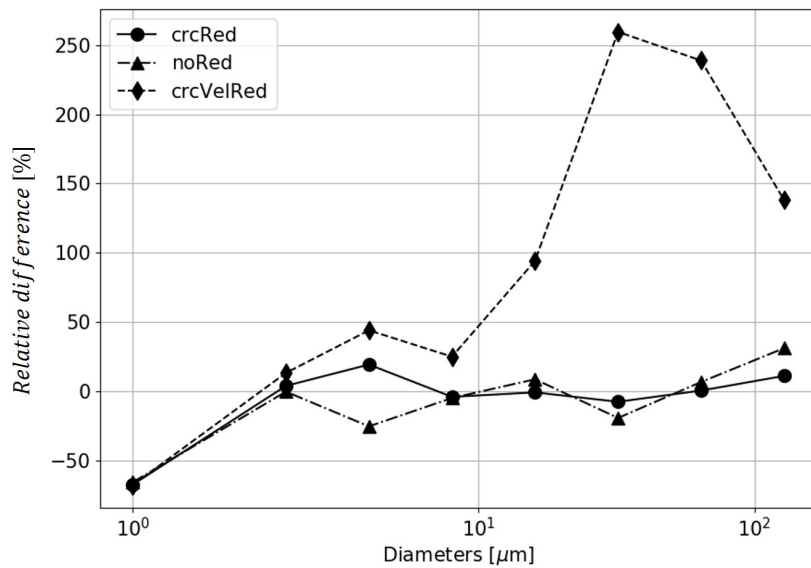


Figure 7: Relative difference between transient and stationary impact efficiencies

tion of particle diameters has been firstly analyzed. Since no significant difference has been found for the impacts on the vane due to the low degree of unsteadiness in the statoric row, the results are here reported only for the rotating cascade. In Fig. 7 the outcomes are presented by means of the percentage difference in the impact number on the blades between each of the steady state simulations and the transient results. Of the three techniques proposed, the *crcRed* is the one that best describes the average behavior of the particles through the interface between the stationary and the rotating component, thus representing the analog of the mixing-plane theory of continuous flows applied to the discrete phases. As can be noted, the impact efficiencies of the *crcRed* are within a 20% difference relative to the transient ones everywhere except for the smallest particles ($1\mu m$). For this diameter, the impacts number is more than doubled with respect to the steady simulation. This discrepancy is also present for the other two methods (*noRed* and *crcVelRed*), which are less accurate in reproducing transient results. This result is somewhat in contrast with the findings of Prenter et al. (2017), who stated that impact efficiency for smaller diameters is better captured with the *crcRed*. This disagreement can be due to the different geometry and operating conditions of the component considered as a reference. Furthermore, this patterns is attributed to the unsteady effects of the wakes and rows interactions, which are propagated in transient simulations and canceled in the steady ones. Indeed, the trajectory of the smallest particles that gravitate in the wake and low-velocity regions is significantly affected by the unsteady transport operated by the continuous phase. On the other hand, larger particles are less influenced by the fluid drag, and their time-averaged behaviour is well captured by the evening out effect pertaining to the circumferential redistribution (*crcRed*). To have also local results from the comparison, impact areas of transient and *crcRed* simulations have been analyzed. For this purpose, the same diameter intervals used for the comparison in the previous section have been kept. The outcomes are reported in Fig. 8. As can be seen from the figure, the impact pattern is closely related for the two frameworks, although some remarkable differences are present for lower diameters. In the transient computation, highly localized impact zones appear in proximity of the blade hub, which are not captured by the *crcRed* computation. The authors impute these discrepancies to the capability of the transient simulation to capture complex unsteady interactions between vane and blade wakes and secondary flows. Such a feature reflects on low-inertia particles, whose impacts are governed by diffusive effects in proximity of solid walls. Indeed, an accumulation of these

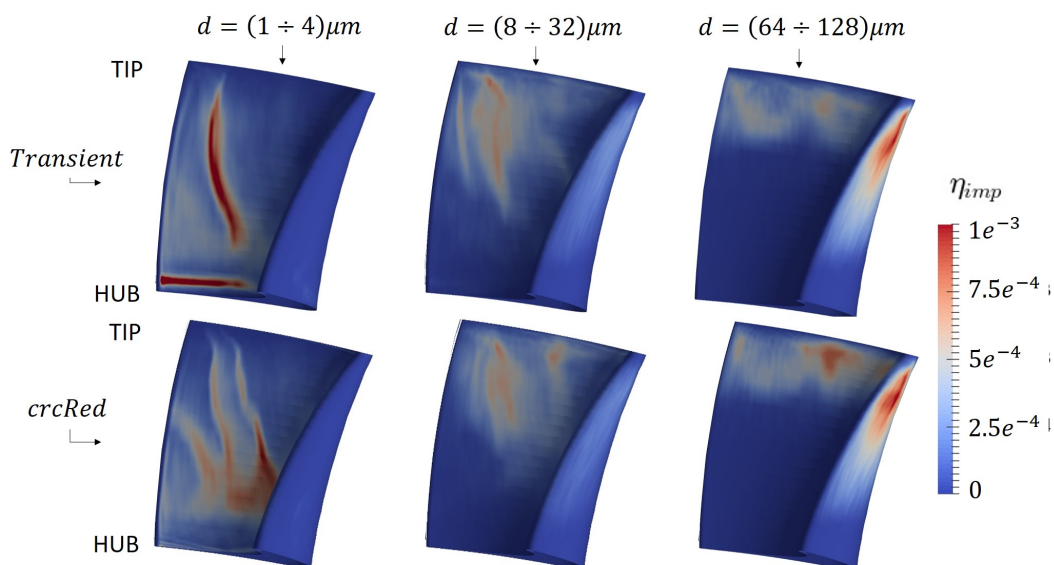


Figure 8: Comparison between impact areas of transient and *crcRed* simulations

particles in the rotor hub region was found in the unsteady simulation causing the greater number of impacts. Moreover, Oliani et al. (2020) showed that different secondary flows patterns can promote or reduce impacts and deposition near the endwalls of nozzle guide vanes. Conversely, particles with a high inertia appear not to be significantly influenced by unsteady effects.

CONCLUSIONS

In this work, solid particle impacts on a turbine stage are analyzed using a steady mixing plane calculation with three different particle-interface interaction techniques: no redistribution, circumferential redistribution, and circumferential redistribution with mixed-out fluid velocity assignment. The methods generated almost identical results for the vane component, but some significant differences arose for the blade. The various methods yielded different impact efficiencies and impact areas, especially for the *crcRedVel* technique. The authors concluded that, when small diameters are considered, particle treatment at the interface doesn't have a prominent effect from a global-impacts count perspective. When inertial properties become important, the results are dominated by the velocity distribution and the velocity assigned to the particles downstream of the interface becomes the most important factor affecting the particles impact behaviour. Particle circumferential redistribution has proved the most effective way to simulate the reciprocal motion of the two rows. Conversely, the *noRed* technique gives different results between the blades for the whole range of diameters. All the three methods have been compared with a high fidelity transient simulation of the domain. This led to declare the circumferential redistribution as the best technique between the three proposed. No major differences in the impact efficiency and impact areas have been found, except for lower diameters. For smaller particles, the transient simulation provides more localized impact areas, with higher impact efficiencies. The authors impute these discrepancies to particle inertia and the capability of the transient simulation to capture complex unsteady interactions between vane and blade wakes and secondary flows. This work has provided insights into the question of which particle-mixing plane interaction model performs best compared to a high fidelity simulation, and is thus suitable for turbomachinery calculations. Furthermore, these results are not restricted to the specific application, since no particle-wall interaction model was used and because a wide range of diameters has been investigated.

References

- Borm, O., Jemcov, A., and Kau, H. (2011). Density based navier stokes solver for transonic flows. In *6th OpenFOAM workshop*, pages 1–30.
- Corsini, A., Rispoli, F., Sheard, A., and Venturini, P. (2013). Numerical simulation of coal fly-ash erosion in an induced draft fan. *Journal of Fluid Engineering*, 135(8):1–12.
- Elghobashi, S. (1994). On predicting particle-laden turbulent flows. *Applied Scientific Research*, 52:309–329.
- Forsyth, P., Gillespie, D. R. H., McGilvray, M., and Galoul, V. (2016). Validation and assessment of the continuous random walk model for particle deposition in gas turbines engines. In *Proceedings of the ASME Turbo Expo 2016: Turbomachinery Technical Conference and Exposition, GT2016-57332*.
- Ghenaiet, A. (2014). Study of Particle Ingestion Through Two-Stage Gas Turbine. In *Proceedings of the ASME Turbo Expo 2014: Turbomachinery Technical Conference and Exposition, GT2014-25759*.

- Gosman, A. D. and Ioannides, E. (1983). Aspects of computer simulation of liquid-fueled combustors. *Journal of Energy*, 7(6):482–490.
- Jasak, H. and Beaudoin, M. (2011). Openfoam turbo tools: from general purpose cfd to turbomachinery simulations. In *Proceedings of the ASME-JSME-KSME 2011 Joint Fluids Engineering Conference, AJK2011-05015*.
- Leach, K. P. (1983). Energy efficient engine high-pressure turbine component rig performance test report. Technical Report CR-160189, NASA Report.
- Liu, B. Y. H. and Agarwal, J. K. (1974). Experimental observation of aerosol deposition in turbulent flows. *Journal of Aerosol Sciences*, 5(2):145–148.
- Oliani, S., Casari, N., Pinelli, M., Suman, A., and Carnevale, M. (2020). Effect of jets in crossflow in deposition mitigation on full 3d ngv with endwall features. In *Proceedings of the ASME Turbo Expo 2020: Turbomachinery Technical Conference and Exposition, GT2020-15367*.
- Oliani, S., Friso, R., Casari, N., Pinelli, M., Suman, A., and Carnevale, M. (2021). Progress in particle-laden flows simulations in multistage turbomachinery with openfoam. In *Proceedings of the ASME Turbo Expo 2021: Turbomachinery Technical Conference and Exposition, GT2021-59474 - Accepted*.
- Prenter, R., Ameri, A., and Bons, J. P. (2017). Computational simulation of deposition in a cooled high-pressure turbine stage with hot streaks. *Journal of Turbomachinery*, 139(9):091005.
- Reagle, C. J., Delimont, J. M., Ng, W. F., and Ekkad, S. V. (2014). Study of microparticle rebound characteristics under high temperature conditions. *J. Eng. Gas Turbines Power*, 136(1):011501.
- Rispoli, F., Delibra, P., Venturini, P., Corsini, A. and Saavedra, R., and Tezduyar, T., E. (2015). Particle tracking and particle-shock interaction in compressible-flow computations with the v-sgs stabilization and yzb shock-capturing. *Computational Mechanics*, 55(6):1201–1209.
- Suman, A., Kurz, R., Aldi, N., Morini, M., Brun, K., Pinelli, M., and Spina, P. R. (2014). Quantitative computational fluid dynamics analyses of particle deposition on a transonic axial compressor blade - part 1: Particle zones impact. *Journal of Turbomachinery*, 137(2):021009.
- Suzuki, M., Inaba, K., and Yamamoto, M. (2006). Numerical simulation of sand erosion phenomena in rotor/stator interaction of compressor. *Journal of Thermal Science*, 17:125–133.
- Tabakoff, W., Hamed, A., and Metwally, M. (1991). Effect of Particle Size Distribution on Particle Dynamics and Blade Erosion in Axial Flow Turbines. *Journal of Engineering for Gas Turbines and Power*, 113(4):607–615.
- Thulin, R. D., Howe, D. C., and Singer, I. D. (1982). High-pressure turbine detailed design report. Technical Report CR-165608, NASA Report.
- Yang, H. and Boulanger, J. (2012). The Whole Annulus Computations of Particulate Flow and Erosion in an Axial Fan. *Journal of Turbomachinery*, 135(1):011040.
- Zagnoli, D., Prenter, R., Ameri, A., and Bons, J. P. (2015). Numerical study of deposition in a full turbine stage using steady and unsteady methods. In *Proceedings of the ASME Turbo Expo 2015, GT2015-43613*.